Journal of Solid State Chemistry **144,** 175–180 (1999)
Article ID jssc.1999.8143, available online at http://www.idealibrary.com on IDEAL®

Lanthanum and Praseodymium Bromide Pnictides. A Convergence of Interstitial Chemistry in Cluster Halides and Intermetallic Pnictides

Elizabeth A. Jensen, Laura M. Hoistad, and John D. Corbett

Department of Chemistry, Iowa State University, Ames, Iowa 50011

Received August 24, 1998; in revised form December 18, 1998; accepted December 22, 1998

Reactions of metal *R*, RBr_3 (*R* = La, Pr), and pnictogen *Pn* (P, As, Sb, Bi) at 900–1000°C provide a new series of condensed cluster products, either cubic R_3Br_3Pn or hexagonal R_5Pn_3Br, but not both for the same *Pn*. Syntheses and lattice dimensions for all eight examples are reported. Cubic R_3Br_3Pn results with interstitial P or As (Ca_3I_3P type, $I4_132$ (No. 214), $Z = 8$), whereas hexagonal P_5Pn_3Br is formed for *Pn* = Sb, Bi with interstitial Br (stuffed Mn_5Si_3 type), a new range of composition for these compounds. The latter structure for La_5Sb_3Br was refined by single-crystal X-ray diffraction data ($P6_3/mcm$ (No. 193), $Z = 2$, $a = 9.602(2)$ Å, $c = 6.7331(3)$ Å, $R(F)/R_w = 1.7/2.0\%$). Features that determine the formation of a particular set of compounds in each structure type are discussed. © 1999 Academic Press

1. INTRODUCTION

A large quantity of research on rare-earth metal (*R*) cluster and condensed cluster halides (*X*) has been carried out in the past 20 years. This has revealed a large number of compounds in which characteristic R_6X_{12}-type clusters may be either discrete or condensed in one, two, or three dimensions into oligomers or, more often, infinite arrays. Substantially all of these require an interstitial atom (*Z*) within each cluster unit for stability. The interstitial atoms may be nonmetals, e.g., B, C, N, Si, or one of many transition metals, i.e., Mn–Cu, Ru–Pd, Re–Au. Stoichiometries for binary phases range from *RXZ* in condensed systems to $R_7X_{12}Z$ with discrete clusters (1, 2). The varieties of structures expand considerably when quaternary alkali-metal derivatives are included (3). Another large family of discrete cluster halides that requires interstitials was encountered first for zirconium, but virtually no isostructural relatives exist among the rare-earth element halides because of the substantially different stoichiometries required to meet basically the same electronic rules for cluster stability (2, 4). Chemistries in the neighboring chalcogenide cluster systems are only distantly related, e.g., as the Chevrel phases.

One cluster halide and structure type we are interested in presently is that of R_3Br_3Pn, a three-dimensional array of condensed clusters known first for Gd_3Cl_3C (5), then for R_3I_3Z, *R* = La, Pr; *Z* = Os, Ir, Pt (6) and Pr_3Br_3Z, *Z* = Co, Os, Rh, Ir, Pt (7). These occur in the cubic Ca_3I_3P structure type, basically a stuffed NaCl derivative (8) and, in contrast, a valence compound. The 3D network is built from *Z*-centered clusters that each share three nonadjacent edges with other clusters.

A widely different family of compounds that shares only the characteristic of a diverse interstitial chemistry has been established and characterized in intermetallic systems. The host binaries all have a common A_5B_3 stoichiometry and an Mn_5Si_3-type structure, the important part of which is a confacial $A_{6/2}B_{6/2}$ chain of trigonal antiprisms of *A* with the shared faces bridged by *B*. These are basically all electron-rich and metallic. The binary examples are widespread, and for the rare-earth elements they are known for most of the tetrel (Si–Pb) and pnictogen families (9). These are relevant here because apparently all examples share the characteristic of A_5B_3Z formation with interstitial *Z* centered in each antiprism (9, 10). For example, the ternary La_5Ge_3Z (11) and La_5Pb_3Z (12) series are each known with 18 to 20 different *Z*, the last spanning many of the lighter half of the main-group elements as well as the later 3*d* elements. Most of these products are still metallic and not electron precise. On the other hand, the known R_5Pn_3 pnictide hosts are virtually uninvestigated with respect to their *Z* chemistry other than R_5Pn_3H for *R* = Eu, Yb (13).

Our synthetic explorations of *R*–Br–*Pn* systems (*R* = La, Pr) for new cluster halide chemistry have led to a surprising confluence of these two very different areas of interstitial chemistry with Br vs *Pn* interstitials. The cubic R_3Br_3 network is stabilized by either P or As, new interstitials for rare-earth-metal halide chemistry, while the heavier Sb and Bi become part of the R_5Pn_3 host with Br as the interstitial in hexagonal (and presumably metallic) R_5Pn_3Br phases. At first, this might be viewed as a result of only a change in size of *Z*, but the two types of compounds formed are

0022-4596/99 $30.00

fundamentally different. Though both involve some degree of *R*–*R* bonding, the cluster halides are more salt-like while the R_5Pn_3Z members are more intermetallic, so we are comparing the addition of R–Pn bonding in a *R*–Br condensed cluster host in the first type with new *R*–Br bonding in a stable R_5Pn_3 framework in the second.

2. EXPERIMENTAL

2.1. Syntheses

All reagents and products were stored and handled in a nitrogen-filled glove box because of their sensitivity to oxygen and moisture. The rare-earth metals came from Ames Lab ($\geq 99.99\%$ purity), and any surface films (oxides or "tarnish") were scraped off before use. Phosphorus (Aldrich, 5–9's), As (Aldrich, 6–9's), Sb (Alfa, 5–9's), and Bi (AESAR, 6–9's) were used as received. $LaBr_3$ and $PrBr_3$ were prepared from the oxides by the ammonium halide method (14) and purified by vacuum sublimation in contact with only Ta (15). Typically, $\sim$250 mg of reactants were loaded into Nb tubes that had previously been cleaned, crimped, and welded on one end. The open ends of the tubes were then tightly crimped, arc-welded under argon, and sealed into well-evacuated, baked fused silica jackets before being heated in the furnace. Phases were identified and yields were estimated visually from Guinier powder diffraction patterns of the products through routine comparisons with calculated patterns, as regard to both line positions and intensities. Powder patterns were also used to determine the lattice parameters of the new phases listed in Table 1 via least squares refinement of line positions relative to Si (NIST) added as an internal standard.

During the initial explorations, many wide-ranging stoichiometries and reaction conditions were tried. *R*OBr was the most common unwanted product, appearing in almost every powder pattern, sometimes as the only impurity. This originated from adventitious water (and perhaps even O_2), mostly as evolved from the fused silica on heating.

For La_3Br_3P, the best results were obtained from mixtures loaded near this stoichiometry (yields 85–100%) and heated to 900–1000°C for 3–4 weeks followed by slow cooling to room temperature (10°C/h). Continued heating at 800–850°C for 4 weeks did not improve yields. Lower yields were obtained when other reactant ratios were tried, while the binary compounds LaP and $LaBr_3$ appeared in the powder patterns of the products at the extremes. The stuffed-Mn_5Si_3 structure was never seen, even when the La_5P_3Br stoichiometry was loaded.

The synthesis of the corresponding arsenide in 80–90% yields was accomplished similarly at 900–950°C. A small amount of $AlBr_3$ in the reaction (as a transporting agent for $LaBr_3$ (16)) produced 85% yields at 850°C after 6 weeks. Other stoichiometries and similar reaction conditions gave lower yields (5–75%) and other phases, commonly $LaBr_3$ and LaAs when well off composition. The hexagonal structure was never seen, even when the stoichiometry La_5As_3Br was loaded. Some weak lines in several complicated patterns were unidentifiable.

La_5Sb_3Br was perhaps the easiest phase of this series to prepare. Even the stoichiometries that produced the cubic phase for Pn = P or As gave instead some of the hexagonal phase with Sb after 950–1000°C for 2–4 weeks. $LaBr_3$, LaOBr, and, less often, LaSb sometimes were found when proportions were varied. Yields of at least 90% could be achieved from the correct reactant proportions. Reactions to gain La_5Bi_3Br were loaded on stoichiometry and resulted in 90% of the intended product plus 10% LaOBr after 2 weeks at 950°C.

Other experiments targeted on La_5Sb_3M (M = Ti, V, Cr, Mn, Fe, Co, Zr) with added KBr, $AlBr_3$, or $LaBr_3$ as potential fluxing or transport agents and run in tantalum at 900 or 950°C for 2 weeks produced La_5Sb_3Br in yields of $\geq 90\%$ (experiments with $AlBr_3$), 40–70% ($LaBr_3$), or 10% (KBr). In all but the $AlBr_3$ trials, the impurities were mixtures of LaSb, $LaSb_2$, LaOBr, and KBr/$LaBr_3$. In some $AlBr_3$ and $LaBr_3$ cases, 5–10% of the powder pattern lines could not be assigned, and it is supposed that these products may have contained other phases incorporating the transition metals.

The analogues Pr_3Br_3Z and Pr_5Z_3Br were loaded on stoichiometry and heated at 950°C for 2 weeks. The yields were high: 90% Pr_3Br_3P, 80% Pr_3Br_3As, $\sim$100% Pr_5Sb_3Br, and 90% Pr_5Bi_3Br, respectively, with the same structure type distribution. The yield of Pr_3Br_3As was lower than for any other phase prepared. PrOBr was the only identifiable impurity, but a few lines (5%) in two of the powder patterns could not be assigned.

TABLE 1
Lattice Constants (Å) and Cell Volumes (Å^3) of Some R_3Br_3Pn and R_5Pn_3Br Phases[a,b]

Composition	Number of lines	*a*	*c*	*V*
La_3Br_3P	42	11.970(2)	—	1715.1(5)
La_3Br_3As	38	12.090(3)	—	1767.2(8)
La_5Sb_3Br	36	9.602(2)	6.7331(3)	537.6(2)
La_5Bi_3Br	47	9.718(5)	6.753(6)	552.3(6)
Pr_3Br_3P	22	11.746(8)	—	1620(2)
Pr_3Br_3As	12	12.02(3)	—	1737(8)
Pr_5Sb_3Br	40	9.378(2)	6.529(4)	497.3(3)
Pr_5Bi_3Br	38	9.528(4)	6.618(7)	520.3(6)

[a] R_3Br_3Pn, $I4_132$, No. 214, $Z = 8$; R_5Pn_3Br, $P6_3/mcm$, No.193, $Z = 2$.
[b] Dimensions from least-squares refinement of Guinier powder diffraction pattern with Si as an internal standard; $\lambda = 1.54056$ Å, 23°C.

2.2. Crystallography

Laue photographs were used to determine the suitability of possible crystals of these phases. Although the powder patterns showed large amounts of the target products, the only usable crystals came from a reaction that had been loaded for La_5Sb_3Cr with $LaBr_3$ added. Later experiments in which no Cr was present resulted in an identical powder pattern, so it was possible to identify the irregular black crystal as La_5Sb_3Br. A crystal was mounted in a thin-walled glass capillary and sealed off, and diffraction data were collected at room temperature with graphite-monochromated Mo$K\alpha$ radiation on a Rigaku AFC6R diffractometer. Routine indexing and cell reduction readily gave a primitive hexagonal cell. The 2027 reflections measured without condition up to $2\theta = 50^\circ$ led, after an absorption correction based on four ψ-scans, to 171 unique reflections ($R_{av} = 5.2\%$). Systematic absences indicated three possible space groups: acentric $P6_3cm$ (No. 185) and $P6c2$ (No. 188) and centric $P6_3/mcm$ (No. 193). The structure was solved by direct methods (17) and refined in the expected centric group with the program TEXSAN (18). Isotropic refinements converged at $R(F) = 3.4\%$ and $R_w = 4.0\%$ and anisotropically at $R = 1.7\%$ and $R_w = 2.0\%$. The largest residual peak in the final difference map was 0.94 e/Å^3. A summary of the crystallographic and refinement parameters are in Table 2, and atomic positional and displacement parameters are given in Table 3. Structure factor data are available from J.D.C.

TABLE 2
Summary of Data Collection and Refinement Parameters for La_5Sb_3Br[a]

Empirical formula	La_5Sb_3Br
Formula weight	1139.7
Crystal size (mm); habit	$0.1 \times 0.2 \times 0.2$; black, irregular
Space group,[a] Z	$P6_3/mcm$ (No. 193), 2
$D_{calc.}$, g/cm^3	7.04
Diffractometer	Rigaku AFC6R
Radiation, λ (Å)	Mo$K\alpha$, 0.71069, graphite-monochromated
μ, cm^{-1} (Mo$K\alpha$)	305.85
Temperature, °C	23
Octants measured	$h, \pm k, \pm l$
Scan mode	ω–2θ
$2\theta_{max}$, °	50
Total reflections measured, R_{av} (%)	2027, 5.2
Observed reflections ($I \geq 3\sigma_I$)	1467
Unique reflections ($I \geq 3\sigma_I$)	171
Variables	14
Relative transmission coefficient range	0.763–1.000
Residuals, R; R_w[b]	1.7; 2.0
Goodness of fit	1.82
$(\Delta\rho)_{max}$, $(\Delta\rho)_{min}$, e/Å^3	0.94, −2.1
Secondary ext. coeff. (10^{-7})	8.7 (4)

[a] Lattice parameters in Table 1.
[b] $R = \sum||F_o| - |F_c||/\sum|F_o|$.
[c] $R_w = [\sum w(|F_o| - |F_c|)^2/\sum w(F_o)^2]^{1/2}$; $w = [\sigma(F)]^{-2}$.

TABLE 3
Positional and Thermal Parameters for La_5Sb_3Br

Atom	x	y	z	B_{eq} (Å^2)[a]	U_{11}[b]	U_{22}	U_{33}
La1	$\frac{2}{3}$	$\frac{1}{3}$	0	0.57(3)	0.0060(5)	0.0081(8)	0.0094(5)
La2	0	0.2744(1)	$\frac{1}{4}$	0.60(6)	0.0081(4)	U_{11}	0.0056(6)
Sb	0.3827(1)	x	$\frac{1}{4}$	0.60(7)	0.0068(6)	0.0080(8)	0.0083(6)
Br	0	0	0	0.84(7)	0.0112(8)	U_{11}	0.010(1)

[a] $B_{eq} = (8\pi^2/3)\sum_i\sum_j U_{ij}a_i^*a_j^*a_ia_j$.
[b] $T = \exp[-2\pi^2(U_{11}h^2a^{*2} + U_{22}k^2b^{*2} + U_{33}l^2c^{*2} + 2U_{12}hka^*b^* + 2U_{13}hla^*c^* + 2U_{23}klb^*c^*)]$, $U_{12} = U_{13} = U_{23} = 0$.

3. RESULTS AND DISCUSSION

3.1. R_3Br_3Pn

Although no suitable single crystals of the cubic phase could be found, the powder diffraction line positions and interstices for the black La_3Br_3P, La_3Br_3As, Pr_3Br_3P, and Pr_3Br_3As agreed very well with those calculated with the refined lattice constants (Table 1) for the Ca_3I_3P structure type with positional parameters as refined earlier for Pr_3I_3Pt (6). Trigonal antiprisms ("octahedra") of the rare-earth metal atoms centered by Pt, P, etc., share three nonadjacent edges with neighboring octahedra while the other nine edges are bridged by multiple-functioned bromine atoms. Figure 1 shows the repeat unit, with heavier lines representing shared R–R edges. This building block clearly derives from the well-known noncondensed $R_6X_{12}Z$-type clusters. In the present cases, a P or As atom occupies the center of each octahedron. The sharing creates a three-

TABLE 4
Important Interatomic Distances (Å) and Angles (°) in La_5Sb_3Br

La1–La1	3.3666(2)	La1–La1–La2	64.434(7)	La2–Br–La2	86.25(1)[c]
La1–La2	3.8997(9)	La2–La1–La2	66.48(2)		93.75(1)[d]
La1–Sb	3.4334(7)	La1–La2–La1	51.14(1)	Sb–La1–Sb	93.08(3)
La2–Sb	3.281(1)	La1–La1–Sb	60.648(7)	Sb–La2–Br	78.17(2)[a]
La2–Br	3.1269(9)	La2–La1–Sb	52.79(2)[a]	La1–Sb–La2	70.85(2)[a]
La2–La2	4.2753(7)		57.01(1)[b]		68.18(1)[b]
Sb–Sb	4.051(1)	La1–La2–Sb	56.30(1)[a]	La2–Sb–La2	86.25(1)[a]
Br–Br	3.3665(2)		54.81(1)[b]	La1–Sb–La1	58.72(1)

[a] La2 and Sb at $z = 1/4$.
[b] La2 at $z = 1/4$, Sb at $z = -3/4$.
[c] La atoms on same face of an octahedron with different z's.
[d] La at same z.
[e] Diagonal La atoms.

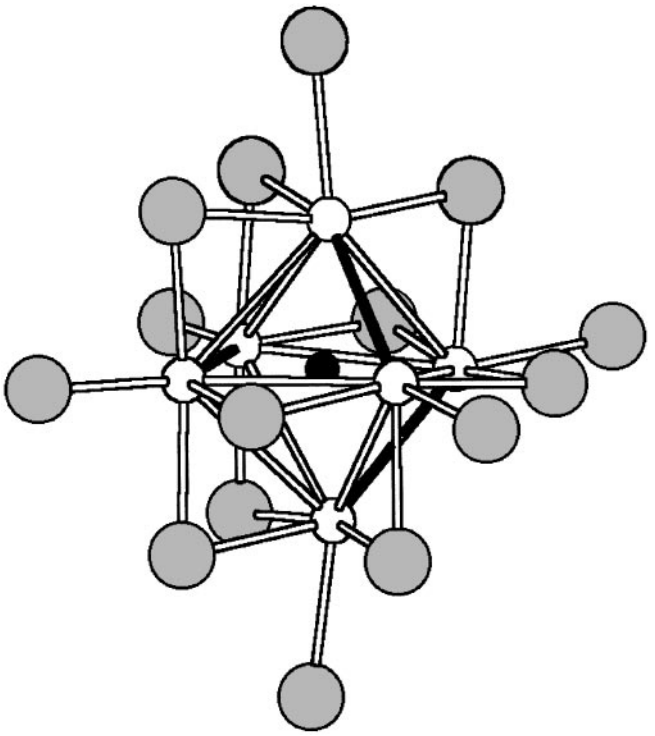

FIG. 1. One octahedral $(R_6Br_9Pn)Br_6$ unit in cubic R_3Br_3Pn, Pn = P or As. Each octahedron shares the three heavier-lined nonadjacent edges not bridged by Br with neighboring octahedra (6).

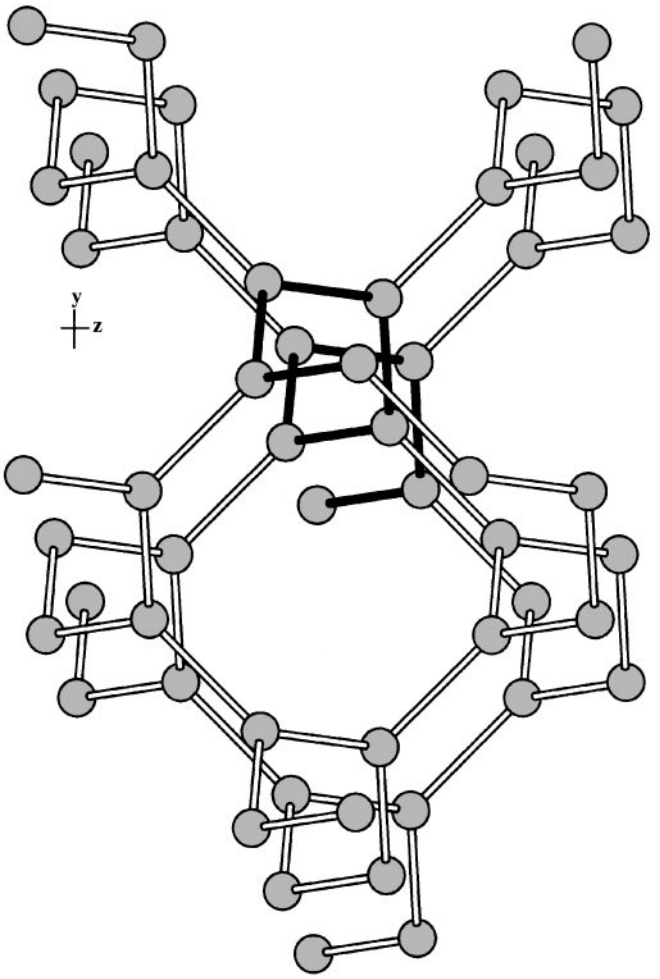

FIG. 2. The 4_1 helices (with one darkened) in the R_3Br_3Pn compounds. Each sphere represents an octahedral unit as in Fig. 1, and the "bonds," the shared edges.

dimensional network of helical 4_1 chains of clusters as shown in Fig. 2, where circles represent clusters and "bonds" the shared edges (6). In contrast, the monoclinic Pr_3Br_3Ru (7) and R_3I_3Z (19) phases with the same stoichiometry consist of $R_6I_{12}Z$ clusters that share both *trans* and some *cis* R–R edges to generate double chains of clusters.

As is usual, the condensed cluster networks in these cubic R_3X_3Z phases afford metallic compounds. This and the bonding have been considered before (6). The way in which the size of the unit cell depends on the identities of the atoms is illustrated by the first two compounds in Table 1. With lanthanum, the cubic lattice dimensions increase by 0.12 Å on changing the P interstitial to As, and the unit-cell volume increases 3%. The same substitution in the smaller Pr compounds results in an increase of 0.27 Å in a while the unit-cell volume increases almost 7%.

3.2. R_5Pn_3Br

One might expect the substitution of Sb for As to result in an even larger cubic lattice constants. However, no examples of R_3Br_3Sb (or R_3Br_3Bi) could be found. Rather, the hexagonal stuffed Mn_5Si_3-type structure results for these R_5Pn_3Br. This ternary structure type for rare-earth metal hosts has been reported earlier for La_5Ge_3Z ($Z = B_x$, C_x, N–Sb, O–Se, Cl, Cr–Zn, Ru, Cd) (11), a similarly large family of La_5Pb_3Z (12), and R_5Pn_3H (R = Eu,Yb) (13). The present bromides represent the first halide analogues of the last hydride family. According to powder diffraction data studies, only the $(La,Pr)_5(Sb,Bi)_3$ binaries have been reported before with presumably unadorned Mn_5Si_3-type structures (9). These all contain infinite chains of confacial trigonal antiprisms ("octahedra") $^1_\infty[R(2)_{6/2}Pn_{6/2}]$ that run along $0, 0, z$ together with 1D linear chains of R atoms, $^1_\infty[R(1)_2Pn_{6/2}]$ along $\frac{1}{3}, \frac{2}{3}, z$, etc., with a short R–R repeat of $c/2$. Both chains involve common Pn. Figure 3 shows the refined result for La_5Sb_3Br. The chains of condensed antiprismatic La_6 are surrounded by one type of Sb atom with three functions, bridging edges of the shared faces of the trigonal antiprisms, bonding exo to $R2$ in neighboring chains (not shown), and defining distorted trigonal antiprisms around $R1$ in the 1D metal strings. Bromine centers every La antiprism. The squat antiprism seen in Fig. 3 and the relatively small c/a value appear to be characteristic

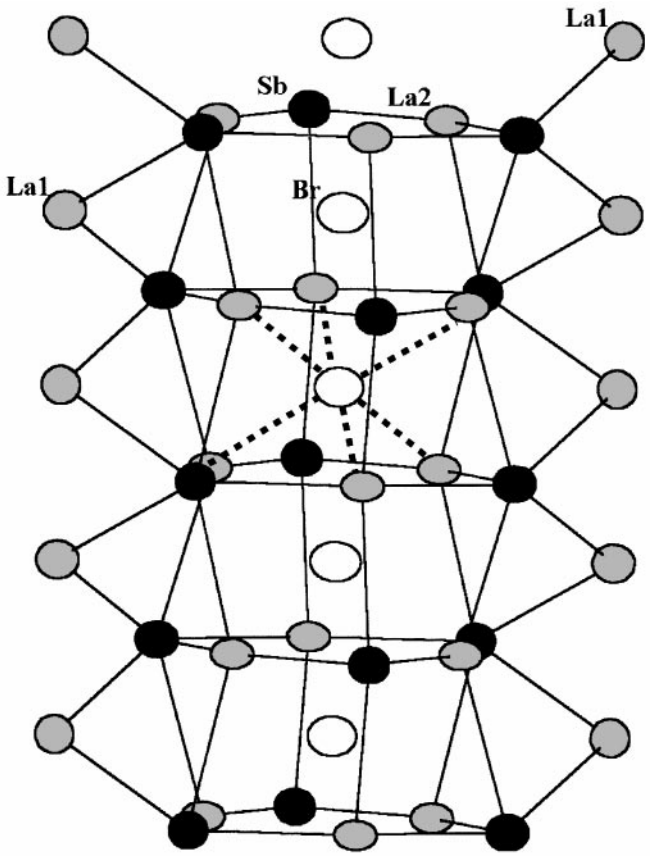

FIG. 3. A view perpendicular to the c axis of hexagonal La_5Sb_3Br ($P6_3/mcm$) showing the chain of confacial trigonal antiprisms of La2 atoms as well as two parallel chains of La1 atoms. The black Sb atoms coordinate both types of gray La atoms while the interstitial Br atoms are shown open (90% probability thermal ellipsoids).

of period 5 main-group elements as they are similar to those found in Zr_5Sn_3Z (20) and Zr_5Sb_3Z (21) with greater numbers of excess electrons than for R_5Pn_3X ($5\cdot3–3\cdot3–1=5$).

The binary La_5Sb_3 has been reported twice before with fairly consistent lattice constants, $a = 9.42(1)$, 9.428 Å and $c = 6.62(1)$, 6.618 Å (22, 23), a necessary but not sufficient condition to ensure that the common impurity Z (H, C, O, etc.) were not present. The addition of the interstitial bromine atom to these supposed binary La_5Sb_3 examples increases both parameters uniformly by $\sim$1.8% and the volume by 5.5% (Table 1) as expected from studies of the known La_5Ge_3Z derivatives, considering that the larger main-group element Sb is present. On the other hand, the consistent literature data for Pr_5Sb_3 (22, 24) afford less believable increases on bromide addition, 1.6% in a but only 0.3% (0.019(6) Å) in c, especially when it is noted that the added bromine Z atoms are still only 3.26 Å ($c/2$) apart along that axis. (Carbon is known to produce such a contraction in c in La_5Ge_3 and La_5Pb_3 (11,12).) Furthermore, comparisons of the present dimensions of the bismuth bromide phases with literature data for R_5Bi_3 require more careful consideration because there is good evidence that at least La_5Bi_3 exists only as a ternary compound (i.e., a Nowotny phase (10)). First, two sets of literature data for the supposed binary La_5Bi_3 (25, 26) differ by 0.045(2) Å (0.5%) in a, but only 0.003 Å (1 σ) in c, good evidence of the presence of interstitial impurities in at least one instance. The larger of these sets of dimensions yields a 2.1% volume increase on incorporation of Br. More importantly, we have been unable to obtain Mn_5Si_3-type La_5Bi_3 after reaction of the pure elements sealed in a tantalum container with heating in an induction furnace under vacuum (to remove H), only the reported anti-Th_3P_3-type La_4Bi_3 appeared (27). Similar studies of Pr_5Bi_3 have not been found, and it is more difficult to judge whether apparent increases of cell lengths and volume of 0.8, 1.0, and 2.6%, respectively, are reasonable. The presence of the large main-group element Bi probably soaks up some of these changes, as it does for the analogous La_5Pb_3Z (12).

An important question regarding these results is why the basic structure type changes so radically with such fairly small changes in the pnictide, i.e., from the cubic La_3Br_3Pn for P and As to hexagonal La_5Pn_3Br with Sb and Bi. Size parallels offer the simplest explanation, especially as far as the known hexagonal R_5Pn_3 binary systems. On this basis, P and As may be too small relative to lanthanum, even before introduction of the large bromine interstitial. A check of Pearson's Handbook (9) reveals that none of the 17 R_5Pn_3 compounds listed with the Mn_5Si_3 structure type contains P, and only two contain As, Eu_5As_3 and Yb_5As_3, both with presumably divalent R. On the other hand, all (but PrAs) of the possible RPn that we saw frequently as alternate products have been reported in the cubic NaCl structure, which is close to the Ca_3I_3P structure but without the interstitial. The implication is that the smaller pnictogens do not form the hexagonal and more intermetallic structure type, with or without an interstitial halogen, particularly with the large R.

Evidence regarding the instability of cubic R_3Br_3Pn for Pn = Sb, Bi is more difficult to find. Perhaps there is only the obvious reason, that La_5Pn_3Br (or other) analogues are more stable. The cubic structure is known for $(La,Pr)_3X_3Z$ for X = Br or I and generally for the later 4d and 5d interstitials (6, 7). Examples of Gd_3Cl_3Z, Z = C, Si are also stable (5). Other prospective combinations have simply not been tested, but this structure is generally not wide-ranging, judging from the results of diverse explorations. Significantly, no rare-earth metal cluster or condensed cluster halide has been found with interstitial elements anywhere near Sb and Bi, and the present P and As are the first reports with these. (The closest were formerly Cu and Si (2).) The elements Sb and Bi would not be expected to generate very strong R–Z bonding in these relatively polar

systems, as contrasted with the more intermetallic R_5Pn_3 hosts. Finally, it should be noted that although a great many $R_xPn_y\mathrm{Br}_z$ compositions were explored in the eight systems studied here, only one other new ternary phase was encountered, a new layered lanthanum bromide phosphide (28).

ACKNOWLEDGMENTS

This research was supported by the National Science Foundation, Solid State Chemistry, via Grant DMR-9510278 and was carried out in the facilities of the Ames Laboratory, U.S. Department of Energy.

REFERENCES

1. A. Simon, Hj. Mattausch, G. J. Miller, W. Bauhofer, and R. K. Kremer, *in* "Handbook on the Physics and Chemistry of Rare Earths" (K. A. Gschneidner and L. Eyring, Eds.), Vol. 15, pp. 191–285. North-Holland. Amsterdam, 1991.
2. J. D. Corbett, *J. Alloys Compd.* **229,** 10 (1985).
3. S. Uma and J. D. Corbett, *Inorg. Chem.* **37,** 1944 (1998).
4. J. D. Corbett, *J. Chem Soc. Dalton Trans.* 575 (1996).
5. E. Warkentin and A. Simon, *Rev. Chim. Miner.* **20,** 488 (1983).
6. P. K. Dorhout, M. W. Payne, and J. D. Corbett, *Inorg. Chem.* **30,** 4960 (1991).
7. R. Llusar and J. D. Corbett, *Inorg. Chem.* **33,** 849 (1994).
8. C. Hamon, R. Marchand, Y. Laurent, and J. Lang, *Bull. Soc. Fr. Miner. Crystallogr.* **97,** 6 (1974).
9. P. Villars and L. D. Calvert, "Pearson's Handbook of Crystallographic Data for Intermetallic Phases," 2nd ed. American Society for Metals International, Materials Park, OH, 1991.
10. J. D. Corbett, E. Garcia, A. M. Guloy, W.-M. Hurng, Y.-U. Kwon, and A. E. Leon-Escamilla, *Chem. Mater.* **10,** 2824 (1998).
11. A. M. Guloy and J. D. Corbett, *Inorg. Chem.* **32,** 3532 (1993).
12. A. M. Guloy and J. D. Corbett, *J. Solid State Chem.* **109,** 352 (1994).
13. E. A. Leon-Escamilla and J. D. Corbett, *J. Alloy Compd.* **265,** 104 (1998).
14. G. Meyer, S. Dötsch, and T. Staffel, *J. Less-Common Met.* **127,** 155 (1987).
15. J. D. Corbett, *Inorg. Synth.* **22,** 31 (1983).
16. G. N. Papatheodorou, *in* "Current Topics in Material Science" (E. Kaldis, Ed.), Vol. 10, p. 258, North-Holland, New York, 1982.
17. G. M. Sheldrick, SHELXS-86, Programs for Structure Determination, Universität Göttingen, Germany, 1986.
18. TEXSAN, Version 6.0, Molecular Structure Corp., The Woodlands, TX, 1990.
19. M. W. Payne, P. K. Dorhout, S.-J. Kim, T. R. Hughbanks, and J. D. Corbett, *Inorg. Chem.* **31,** 1389 (1992).
20. Y.-U. Kwon and J. D. Corbett, *Chem. Mater.* **4,** 1348 (1992).
21. E. Garcia and J. D. Corbett, *Inorg. Chem.* **29,** 3274 (1990).
22. W. Rieger and E. Parthé, *Acta Crystallogr., Sect. B* **24,** 456 (1968).
23. G. Borzone, A. Borsese, A. Saccone, and R. Ferro, *J. Less-Common Met.* **65,** 253 (1979).
24. M. N. Abdusalyanova, O. I. Rahmaton, N. D. Faslyeva, and A. G. Tehuiko, *J. Less-Common Met.* **141,** L23 (1988).
25. K. Yoshihara, J. B. Taylor, L. D. Calvert, and J. G. Despault, *J. Less-Common Met.* **41,** 329 (1975).
26. K. Nomura, H. Hayakawa, and S. Ono, *J. Less-Common Met.* **52,** 259 (1977).
27. E. A. Leon-Escamilla, Ph.D. dissertation, Iowa State University, 1996.
28. E. A. Jensen and J. D. Corbett, unpublished research.